

# Consciousness Energy Healing Treatment: Impact on the Physicochemical and Thermal Characteristics of Folic Acid

Gopal Nayak<sup>1</sup>, Mahendra Kumar Trivedi<sup>1</sup>, Alice Branton<sup>1</sup>, Dahryn Trivedi<sup>1</sup>, Snehasis Jana<sup>2, \*</sup>

<sup>1</sup>Trivedi Global, Inc., Henderson, USA.

<sup>2</sup>Trivedi Science Research Laboratory Pvt. Ltd., Bhopal, India.

## Abstract

Folic acid is essential in the body for the production of DNA and also plays various vital functions within the body. This study on folic acid was done to analyze the results of the Trivedi Effect<sup>®</sup> on its physicochemical and thermal properties with the help of analytical techniques. The method involves dividing the test sample into two parts. The first part was termed as a control sample, and no treatment was given to it; while the second part received the Biofield Energy Treatment remotely by a renowned Biofield Energy Healer, Gopal Nayak and termed as the treated sample. The study revealed that the particle sizes reduced by 7.01% ( $d_{10}$ ), 6.53% ( $d_{50}$ ), 8.37% ( $d_{90}$ ), and 15.99%  $\{D(4,3)\}$ , thus increased the surface area by 1.72%, in the treated sample compared with the control sample. The PXRD data showed changes in the peak intensities and crystallite sizes ranging from -36.81% to 113.41% and -15.79% to 318%, respectively, thus increased in the average crystallite size by 22.55% of the treated sample compared with the control sample. The TGA analysis of the treated sample revealed a 3.94% increase in total weight loss that resulted in the remarkable reduction in the residual amount by 14.99%, in comparison to the untreated sample. The latent heat of fusion ( $\Delta H_{\text{fusion}}$ ) and latent heat of decomposition ( $\Delta H_{\text{degradation}}$ ) were significantly altered by -10.33% and 10.46%, respectively in the treated sample compared to the untreated sample. The study denoted that the Biofield Energy Treatment is a novel approach that could be used to develop some polymorph of folic acid and that might improve its solubility, dissolution, and bioavailability in comparison to the control sample. Hence, the treated folic acid in the nutraceutical/pharmaceutical formulations might be useful concerning better drug performance and efficacy.

**Corresponding author:** Snehasis Jana, Trivedi Science Research Laboratory Pvt. Ltd., Bhopal, India. Tel: +91-022-25811234; Email: [publication@trivedieffect.com](mailto:publication@trivedieffect.com)

**Citation:** Gopal Nayak, Mahendra Kumar Trivedi, Alice Branton, Dahryn Trivedi, Snehasis Jana (2018) Consciousness Energy Healing Treatment: Impact on the Physicochemical and Thermal Characteristics of Folic Acid. International Journal of Nutrition - 3(1):30-42. <https://doi.org/10.14302/issn.2379-7835.ijn-18-2419>

**Keywords:** Folic acid, Consciousness Energy Healing Treatment, The Trivedi Effect<sup>®</sup>, Particle size, PXRD, DSC

**Running title:** Consciousness Energy Healing Treatment on Folic acid

**Received:** Oct 11, 2018

**Accepted:** Oct 24, 2018

**Published:** Oct 25, 2018

**Editor:** Jie Yin, Institute of Subtropical Agriculture & University of Chinese Academy of Sciences, China.

## Introduction

Folic acid (vitamin B<sub>9</sub>) is the name used for a conjugate of 4-aminobenzoic acid and L-glutamic acid *i.e.*, folate [1]. Its biologically active form is tetrahydrofolic acid that acts similar to the cobalamins. Folic acid is important as it helps in the production of deoxyribonucleic acid (DNA) and also plays various vital functions within the body. The folic acid is synthetic form, while its natural form is folate that is found in food. It is generally used in combination with other B vitamins [2]. The important food sources containing folate are cereals, leafy vegetables such as broccoli, spinach, lettuce, *etc.*; fruits such as melons, bananas, lemons, *etc.*; okra, legumes, asparagus, yeast, organ meat, mushrooms, and orange and tomato juice [3, 4].

Folic acid is mainly used in the treatment and prevention of folate deficiency and the other associated complications, such as anaemia and malabsorption due to bowel inability [5]. The use of folic acid is also evident in the prevention of stroke and heart disease, due to its property to reduce homocysteine level in the blood, which might create risk for heart disease. The other uses of folic acid involve the treatment of liver disease, ulcerative colitis, alcoholism, and kidney diseases such as dialysis. It is also used by pregnant women to prevent miscarriage and neural tube defects, such as spina bifida. Some researchers also indicated the use of folic acid in the prevention of colon and cervical cancer. Moreover, folic acid is used for the prevention and treatment of Alzheimer's disease, memory loss, eye disease age-related macular degeneration, age-related hearing loss, aging, sleep problems, osteoporosis, depression, restless leg syndrome, nerve pain, vitiligo, gum infections, muscle pain, and Fragile-X syndrome, which is an inherited disease [6-9]. Folic acid also helps in reducing the side effects of lometrexol and methotrexate drugs and associated problems [10].

The physicochemical properties of the drug are important regarding its absorption, distribution, metabolism, and excretion (ADME) profile and thus, it is advised to improve the biological activities and efficacy of the drug by altering its physicochemical properties [11]. Consciousness Energy Healing Treatment is one among such approaches that could be used in modifying the physical, structural, and thermal properties of the

drugs [12, 13]. The Biofield Energy Healing is widely accepted as an alternative integrative approach that helps in improving the quality of life by correcting the root cause of the diseases [14-16]. A human can harness energy from the universe and can transmit it to any living organism(s) or non-living object(s) around the globe. The object or recipient always receives the energy and responds in a useful way. This process is known as the Trivedi Effect<sup>®</sup>-Biofield Energy Healing Treatment [17, 18]. The Trivedi Effect<sup>®</sup>- Consciousness Energy Healing Treatment has shown its effect on the crops and its productivity, microbes, metals, chemicals, ceramics, nutraceuticals, skin health, bioavailability, bone health, cancer [19-37], *etc.* This study was also designed to establish the physicochemical and thermal properties of the treated folic acid and to determine the impact of the Trivedi Effect<sup>®</sup> on the properties of folic acid as compared to the control one with the help of various analytical techniques.

## Materials and Methods

### *Chemicals and Reagents*

Folic acid was purchased from Alfa Aesar, USA; whereas the remaining chemicals used in the experiments were of analytical grade purchased from India.

### *Consciousness Energy Healing Treatment Strategies*

The folic acid sample used in the study was first divided into two parts. The first part of the samples was not given the Biofield Energy Treatment and considered as the control sample. Besides, the second part of the sample was received the Trivedi Effect<sup>®</sup>-Energy of Consciousness Healing Treatment under standard laboratory conditions for 3 minutes and known as the Biofield Energy Treated folic acid sample. This Biofield Energy Treatment was provided remotely through the healer's unique energy transmission process by a famous Biofield Energy Healer, Gopal Nayak, India, to the test sample. Later on, the control sample was treated with a "sham" healer for comparison purpose. The "sham" healer did not have any knowledge about the Biofield Energy Treatment. Now, the control and Biofield Energy Treated sample were kept in sealed conditions and characterized using modern analytical techniques.

## Characterization

### Particle Size Analysis (PSA)

The particle size analysis of folic acid samples was carried out on Malvern Mastersizer 2000, from the UK with a detection range between 0.01  $\mu\text{m}$  to 3000  $\mu\text{m}$  using wet method [38, 39]. The % change in particle size (d) at below 10% level ( $d_{10}$ ), 50% level ( $d_{50}$ ), 90% level ( $d_{90}$ ), and  $D(4,3)$  was calculated using the following equation 1:

$$\% \text{ change in particle size} = \frac{[d_{\text{Treated}} - d_{\text{Control}}]}{d_{\text{Control}}} \times 100 \quad (1)$$

Where  $d_{\text{Control}}$  and  $d_{\text{Treated}}$  are the particle size ( $\mu\text{m}$ ) of the control and the Biofield Energy Treated folic acid samples, respectively.

The % change in surface area (S) was calculated using following equation 2:

$$\% \text{ change in surface area} = \frac{[S_{\text{Treated}} - S_{\text{Control}}]}{S_{\text{Control}}} \times 100 \quad (2)$$

Where  $S_{\text{Control}}$  and  $S_{\text{Treated}}$  are the surface area of the control and treated folic acid samples, respectively.

### Powder X-ray Diffraction (PXRD) Analysis

The PXRD analysis of control and the Biofield Energy Treated folic acid was performed with the help of Rigaku MiniFlex-II Desktop X-ray diffractometer (Japan) [40, 41]. The average size of individual crystallites was calculated from XRD data using the Scherrer's formula 3:

$$G = k\lambda/\beta\cos\theta \quad (3)$$

Where k is the equipment constant (0.94), G is the crystallite size in nm,  $\lambda$  is the radiation wavelength (0.154056 nm for  $K\alpha_1$  emission),  $\beta$  is the full-width at half maximum (FWHM), and  $\theta$  is the Bragg angle [42].

The % change in crystallite size (G) of folic acid was calculated using the following equation 4:

$$\% \text{ change in crystallite size} = \frac{[G_{\text{Treated}} - G_{\text{Control}}]}{G_{\text{Control}}} \times 100 \quad (4)$$

Where  $G_{\text{Control}}$  and  $G_{\text{Treated}}$  are the crystallite size of the control and treated samples, respectively.

### Thermal Gravimetric Analysis (TGA)/ Differential thermogravimetric analysis (DTG)

TGA/DTG thermograms of the control and the Biofield Energy Treated folic acid were obtained with the help of TGA Q50TA instruments. A sample of 4-15 mg was loaded to the platinum crucible at a heating rate of 10°C/min from 25°C to 1000°C with the recent literature [43]. The % change in weight loss (W) was calculated using the following equation 5:

$$\% \text{ change in weight loss} = \frac{[W_{\text{Treated}} - W_{\text{Control}}]}{W_{\text{Control}}} \times 100 \quad (5)$$

Where  $W_{\text{Control}}$  and  $W_{\text{Treated}}$  are the weight loss of the control and the Biofield Energy Treated folic acid, respectively.

The % change in maximum thermal degradation temperature ( $T_{\text{max}}$ ) (M) was calculated using the following equation 6:

$$\% \text{ change in } T_{\text{max}} (M) = \frac{[M_{\text{Treated}} - M_{\text{Control}}]}{M_{\text{Control}}} \times 100 \quad (6)$$

Where  $M_{\text{Control}}$  and  $M_{\text{Treated}}$  are the  $T_{\text{max}}$  values of the control and treated folic acid, respectively.

### Differential Scanning Calorimetry (DSC)

The DSC analysis of folic acid was performed with the help of DSC Q200, TA instruments. A sample of ~1-5 mg was loaded to the aluminium sample pan at a heating rate of 10°C/min from 30°C to 350°C [43]. The % change in melting point (T) was calculated using the following equation 7:

$$\% \text{ change in melting point} = \frac{[T_{\text{Treated}} - T_{\text{Control}}]}{T_{\text{Control}}} \times 100 \quad (7)$$

Where  $T_{\text{Control}}$  and  $T_{\text{Treated}}$  are the melting point of the control and treated samples, respectively.

The % change in the latent heat of fusion ( $\Delta H$ ) was calculated using the following equation 8:

$$\% \text{ change in the latent heat of fusion} = \frac{[\Delta H_{\text{Treated}} - \Delta H_{\text{Control}}]}{\Delta H_{\text{Control}}} \times 100 \quad (8)$$

Where  $\Delta H_{\text{Control}}$  and  $\Delta H_{\text{Treated}}$  are the latent heat of fusion of the control and treated folic acid, respectively.

### Statistical Analysis

The values were represented as Mean  $\pm$  SEM (standard error of mean) of the independent experiments. For two groups comparison student's  $t$

test was used. Statistically significant values were set at the level of  $p \leq 0.05$ .

## Results and Discussion

### Particle Size Analysis (PSA)

The particle size analysis corresponding to  $d_{10}$ ,  $d_{50}$ ,  $d_{90}$ , and  $D(4, 3)$  of the control and the Biofield Energy Treated sample was done and the results are mentioned in Table 1. It revealed that the particle size distribution of the treated folic acid sample was significantly reduced by 7.01%, 6.53%, 8.37%, and 15.99% at  $d_{10}$ ,  $d_{50}$ ,  $d_{90}$ , and  $D(4, 3)$ , respectively, compared to the control sample.

The decrease in particle size resulted in the increase in specific surface area (SSA) of the treated sample as the SSA was observed as  $1.74 \text{ m}^2/\text{g}$  in the control sample; while it was increased by 1.72% and observed as  $1.77 \text{ m}^2/\text{g}$  in the treated sample. The particle size distribution is important regarding the efficacy and performance of drug within the body in terms of its solubility, dissolution, and bioavailability [11, 44]. The decreased particle size of the treated folic acid that resulted in the increased surface area could be used as an approach to improve the bioavailability and efficacy of drug [45]. Hence, it could be anticipated that the treated folic acid might show better bioavailability profile after the Biofield Energy Treatment when used in the pharmaceutical and nutraceutical formulations in comparison to the untreated sample.

### Powder X-ray Diffraction (PXRD) Analysis

The PXRD diffractograms of the control and treated folic acid samples are shown in Figure 1. The analysis revealed the crystalline nature of both the samples as shown by the sharp and intense peaks present in their diffractograms. The further analysis was done (Table 2) to determine any changes in the Bragg's angles, relative peak intensities, and crystallite sizes corresponding to the characteristic peaks of the treated sample as compared to the control sample.

The results revealed that the Bragg's angles of the peaks present in the diffractogram of the treated sample were slightly altered compared to the control sample; however the major alteration was observed in the peak at  $2\theta$  equals to  $12.29^\circ$  in the control sample that was observed at  $2\theta$  equals to  $13.07^\circ$  (entry no. 2)

in the treated sample's diffractogram. Besides, the peak intensities of the treated folic acid sample were altered ranging from -36.81% to 113.41%; and the crystallite sizes were varied ranging from -15.79% to 318%, compared to the control sample. The major alteration was also observed in the average crystallite size as it was observed as 152.68 nm in the treated sample, which was significantly increased by 22.55% in comparison to the control sample (124.58 nm). The alterations in the crystalline structure, as well as crystal morphology of drugs have been reported previously by using the Biofield Energy Treatment. It is supposed that the Consciousness Energy Healing Treatment might form a new polymorph of the compound by changing the peak intensities and crystallite sizes [46, 47]. Such novel polymorph of folic acid might possess better bioavailability and drug profile compared with the untreated sample.

### Thermal Gravimetric Analysis (TGA)/ Differential Thermogravimetric Analysis (DTG)

The analysis of the thermal stability of both the samples, *i.e.*, the control and treated samples were done using TGA/DTG technique. The TGA thermograms of both the samples are presented in Figure 2 and the results (Table 3) revealed that the total weight loss of the treated folic acid during thermal degradation was increased by 3.94% as compared to the control sample. Therefore, the residual amount remaining after the degradation of the Biofield Energy Treated sample was observed to be significantly reduced by 14.99% in comparison to the control folic acid sample. Hence, it indicated the increased thermal degradation of the treated sample compared to the untreated folic acid sample.

The DTG analysis of both the samples showed four peaks in their respective thermograms (Figure 3). It was observed that the maximum thermal degradation temperatures ( $T_{\text{max}}$ ) in the treated sample corresponding to 1<sup>st</sup>, 2<sup>nd</sup> and 3<sup>rd</sup> peaks were increased by 1.23%, 0.68%, and 2.89%, respectively compared to the control sample. However, the treated sample showed a slight reduction in the  $T_{\text{max}}$  of the 4<sup>th</sup> peak by 1.39% in comparison to the control folic acid sample. Thus, the overall analysis revealed improvement in the thermal degradation temperature of the Biofield Energy Treated

Table 1. Particle size distribution of the control and the Biofield Energy Treated folic acid.

Parameter	d <sub>10</sub> (µm)	d <sub>50</sub> (µm)	d <sub>90</sub> (µm)	D(4,3) (µm)	SSA(m <sup>2</sup> /g)
Control	1.71	4.75	17.81	8.69	1.74
Biofield Treated	1.59	4.44	16.32	7.30	1.77
Percent change* (%)	-7.01	-6.53	-8.37	-15.99	1.72

d<sub>10</sub>, d<sub>50</sub>, and d<sub>90</sub>: particle diameter corresponding to 10%, 50%, and 90% of the cumulative distribution, D(4,3): the average mass-volume diameter, and SSA: the specific surface area. \*denotes the percentage change in the Particle size distribution of the Biofield Energy Treated sample with respect to the control sample.

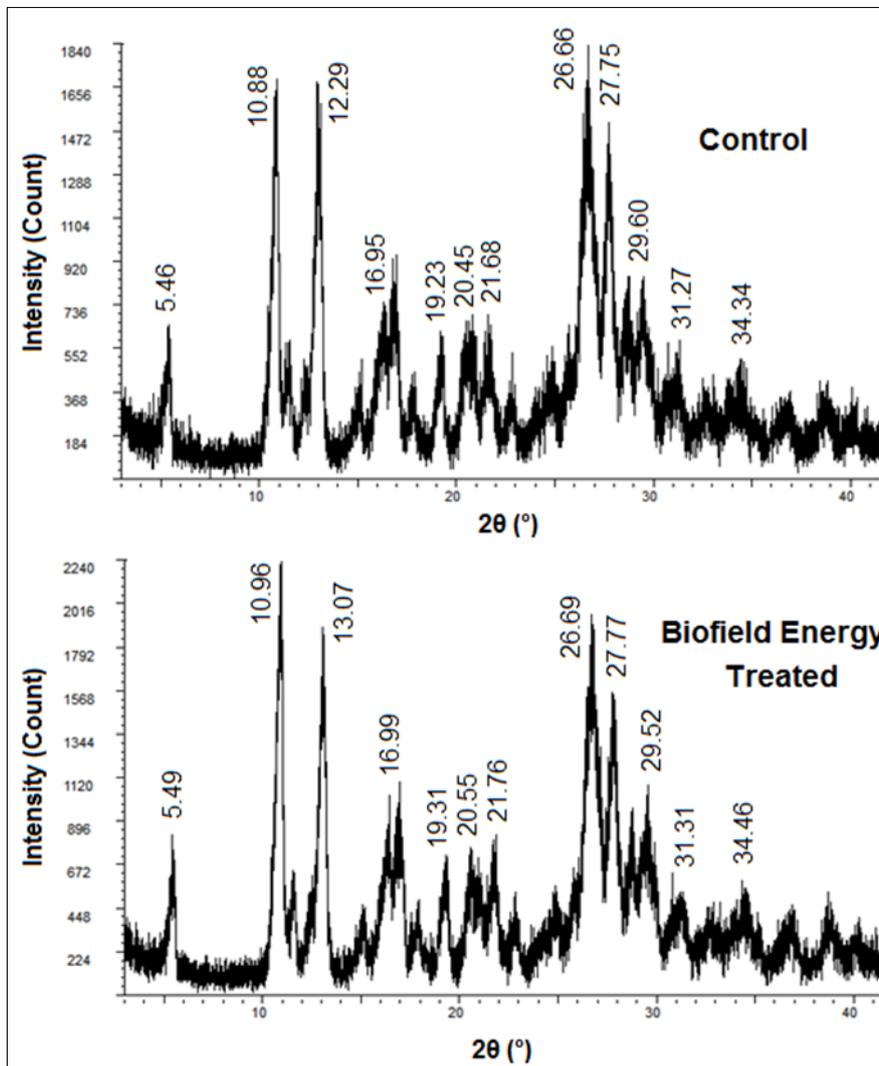


Figure 1. PXRD diffractograms of the control and the Biofield Energy Treated folic acid.

Table 2. PXRD data for the control and the Biofield Energy Treated folic acid.

Entry No.	Bragg angle ( $^{\circ}2\theta$ )		Intensity (cps)			Crystallite size (G, nm)		
	Control	Treated	Control	Treated	% change*	Control	Treated	% change*
1	5.46	5.49	307	194	-36.81	99	240	142.42
2	10.88	10.96	373	559	49.87	195	203	4.1
3	12.29	13.07	261	557	113.41	50	209	318
4	16.95	16.99	357	491	37.54	84	78.1	-7.02
5	19.23	19.31	91	118	29.67	227	218	-3.96
6	20.45	20.55	188	237	26.06	114	96	-15.79
7	21.68	21.76	112	117	4.46	181	212	17.13
8	26.66	26.69	593	870	46.71	110	110	0
9	27.75	27.77	253	470	85.77	199	168	-15.58
10	29.6	29.52	565	436	-22.83	42	92	119.05
11	31.27	31.31	109	145	33.03	103	120	16.5
12	34.34	34.46	111	146	31.53	91	86	-5.49
13	Average crystallite size $\pm$ SEM					124.58 $\pm$ 17.57	152.68 $\pm$ 17.65	22.55

\*denotes the percentage change in the crystallite size of the Biofield Energy Treated sample with respect to the control sample, SEM: standard error of the mean.

Table 3. TGA/DTG data of the control and the Biofield Energy Treated samples of folic acid.

Sample	TGA		DTG { $T_{max}$ ( $^{\circ}C$ )}			
	Total weight loss (%)	Residue %	Peak 1	Peak 2	Peak 3	Peak 4
Control	79.19	20.81	107.71	247.93	433.78	709.61
Biofield Energy Treated	82.31	17.69	109.04	249.63	446.32	699.77
% Change*	3.94	-14.99	1.23	0.68	2.89	-1.39

\*denotes the percentage change of the Biofield Energy Treated sample with respect to the control sample,  $T_{max}$  = the temperature at which maximum weight loss takes place in TG or peak temperature in DTG.

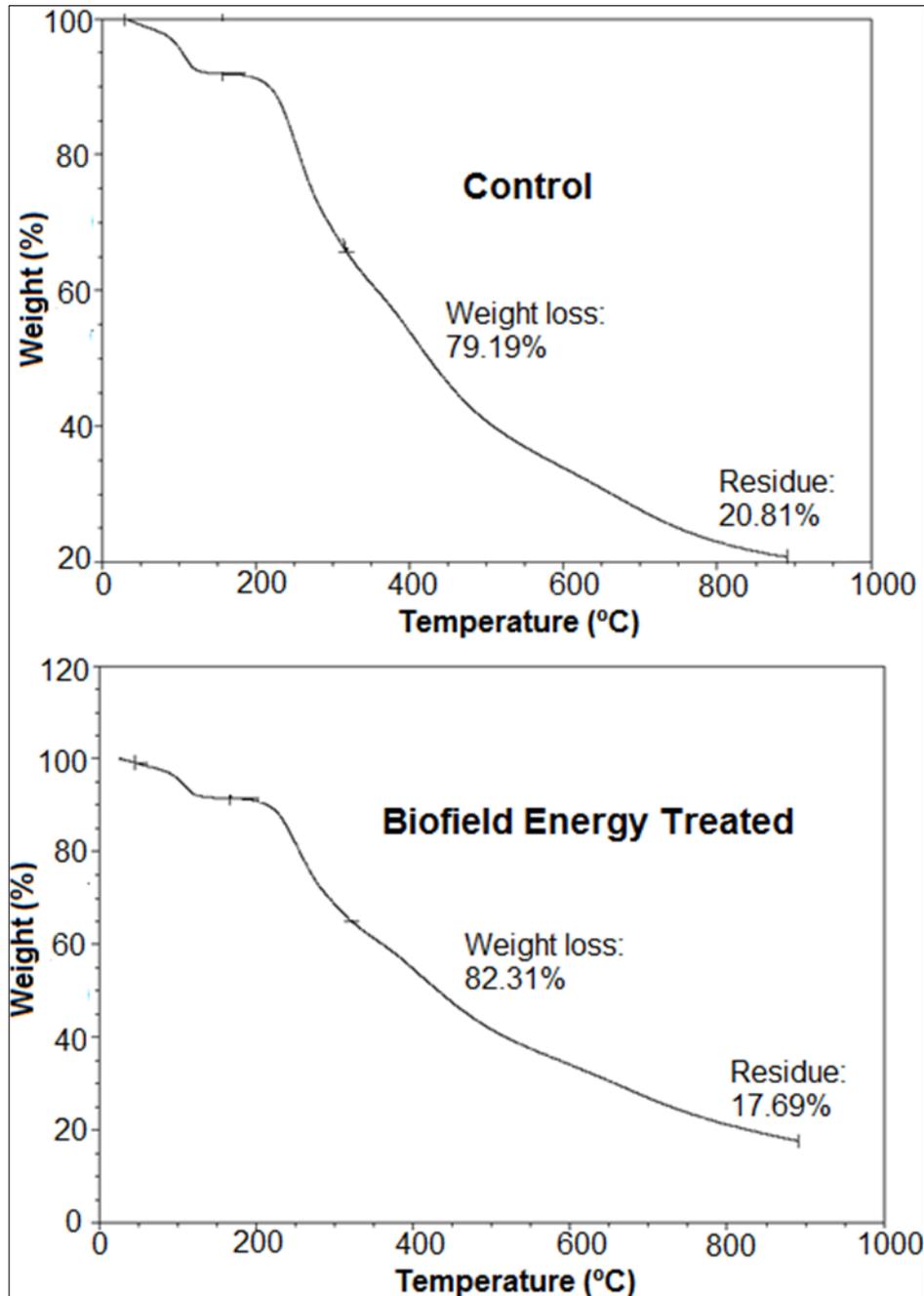


Figure 2. TGA thermograms of the control and the Biofield Energy Treated folic acid.

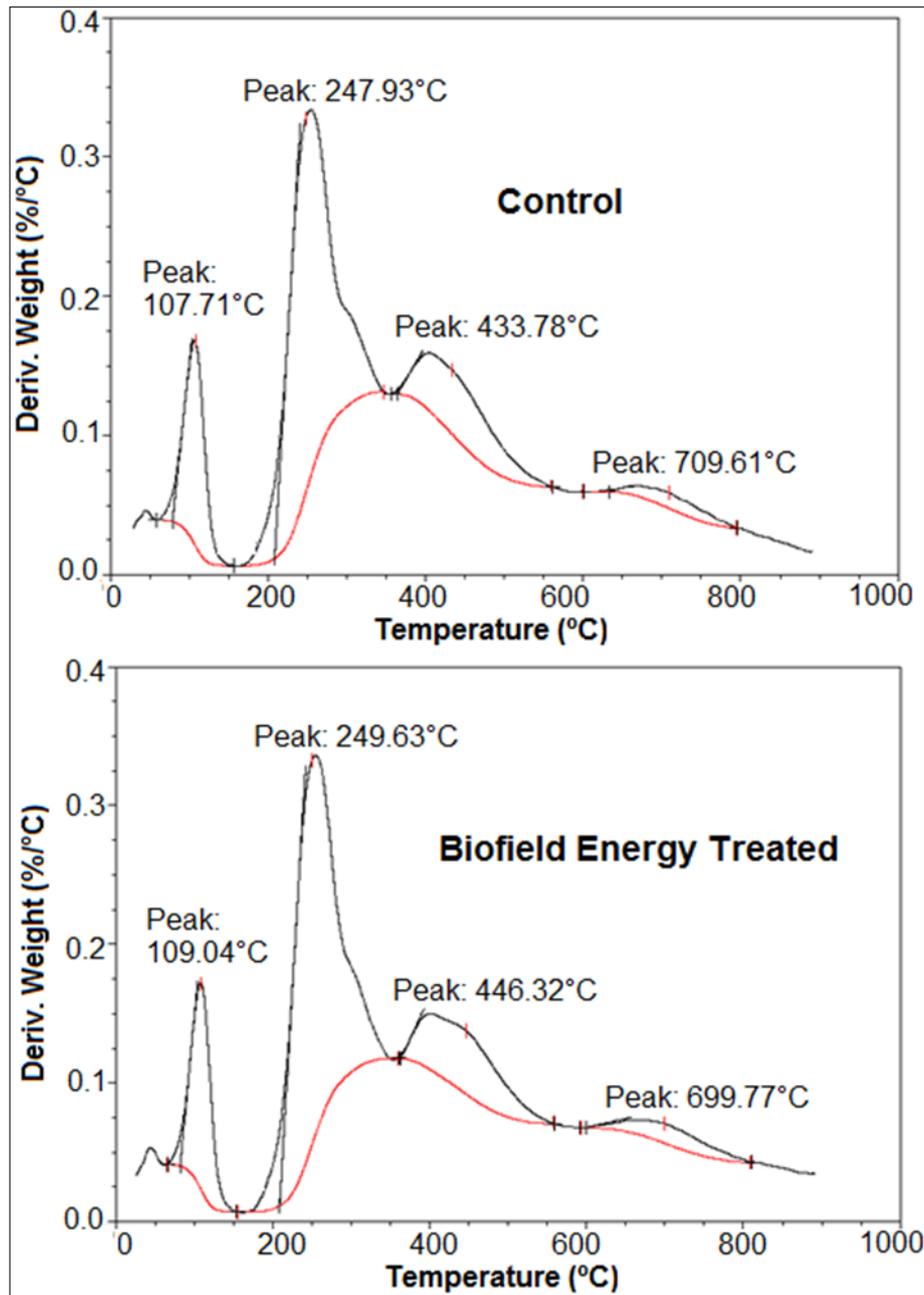


Figure 3. DTG thermograms of the control and the Biofield Energy Treated folic acid.

sample compared with the control sample.

#### *Differential Scanning Calorimetry (DSC) Analysis*

The DSC analysis was used in this study to determine the thermal behaviour of the samples such as melting, crystallization temperature, *etc.* [48]. According to the scientific literature, the heating of folic acid causes the breaking of the "Glu" moiety first at  $\sim 180^{\circ}\text{C}$ , after which the degradation of pterin and PABA takes place in an overlapping form. Moreover, upon further heating, there was the loss of amide and acid functionalities of the compound at  $\sim 195^{\circ}\text{C}$ , and heating beyond that degrades the crystalline folic acid in the form of amorphous one above  $200^{\circ}\text{C}$  [49].

There were two peaks in the DSC thermograms of the control and treated sample (Figure 4) and the further analysis related to peak temperature and enthalpy change for both the samples was presented in Table 4. The first peak *i.e.*, endothermic in nature, was observed in both the thermograms that indicated the melting of the control and treated sample. The peak temperature for the treated sample was observed to be increased by 2.42%, along with 10.33% reduction in the latent heat of fusion ( $\Delta H_{\text{fusion}}$ ) compared to the control sample (Table 4). Besides, the second peak in both the samples is broad and exothermic in nature and might indicate the degradation of the samples after further heating. The analysis showed that the degradation temperature of the treated sample was at  $231.11^{\circ}\text{C}$ , *i.e.*, reduced by 1.60% in comparison to the control sample ( $234.86^{\circ}\text{C}$ ). Moreover, the latent heat of degradation ( $\Delta H_{\text{degradation}}$ ) corresponding to this peak of the treated folic acid sample was significantly increased by 10.46% in comparison to the control sample (Table 4).

The DSC results denoted that the thermal properties of treated folic acid were altered after the Biofield Energy Treatment that might occur due to some changes in the crystallization structure [50] of the treated folic acid as evident in the PXRD analysis. Hence, it is presumed that the Biofield Energy Treated folic acid might be more stable against heating compared to the untreated sample.

#### **Conclusions**

The study of Biofield Energy Treated folic acid revealed

the significant effect of the Trivedi Effect<sup>®</sup>-Consciousness Energy Healing Treatment on its physicochemical and thermal properties. It indicated the significant changes in the particle size distribution of folic acid after the Biofield Energy Treatment. The treated sample showed reduced particle size at  $d_{10}$ ,  $d_{50}$ ,  $d_{90}$ , and  $D(4,3)$  by 7.01%, 6.53%, 8.37%, and 15.99%, respectively compared to the control sample. The decrease in particle size of the Biofield Energy Treated sample causes an increase in the specific surface area by 1.72% compared to the control folic acid sample. The PXRD diffractograms indicated significant alterations in the peak intensities and crystallite sizes ranging from -36.81% to 113.41% and -15.79% to 318%, respectively, compared to the untreated sample. The average crystallite size of the treated folic acid sample was found to be increased by 22.55% after the Biofield Energy Treatment in comparison to the control sample. The TGA data showed the increase in total weight loss of the Biofield Energy Treated sample by 3.94% that resulted in significant reduction in residue weight by 14.99%, compared to the control sample. The treated sample showed that the melting temperature and  $\Delta H_{\text{fusion}}$  were altered by 2.42% and -10.33%, respectively; while the degradation temperature and  $\Delta H_{\text{degradation}}$  were changed by -1.60% and 10.46%, respectively compared to the untreated folic acid sample. The overall data indicated that the Trivedi Effect<sup>®</sup>-Consciousness Energy Healing Treated folic acid formed a new polymorph that may improve the solubility, dissolution, absorption, and bioavailability along with thermal stability compared to the untreated sample. Thus, it could be presumed that the Biofield Energy Treated folic acid would be more efficacious in the pharmaceutical/nutraceutical preparations regarding the prevention and treatment of several diseases such as Alzheimer's disease, memory loss, eye disease, age-related macular degeneration, age-related hearing loss, aging, allergic diseases, sleep problems, osteoporosis, depression, restless leg syndrome, nerve pain, vitiligo, gum infections, muscle pain, Fragile-X syndrome, *etc.*

#### **Acknowledgements**

The authors are grateful to Central Leather Research Institute, SIPRA Lab. Ltd., Trivedi Science,

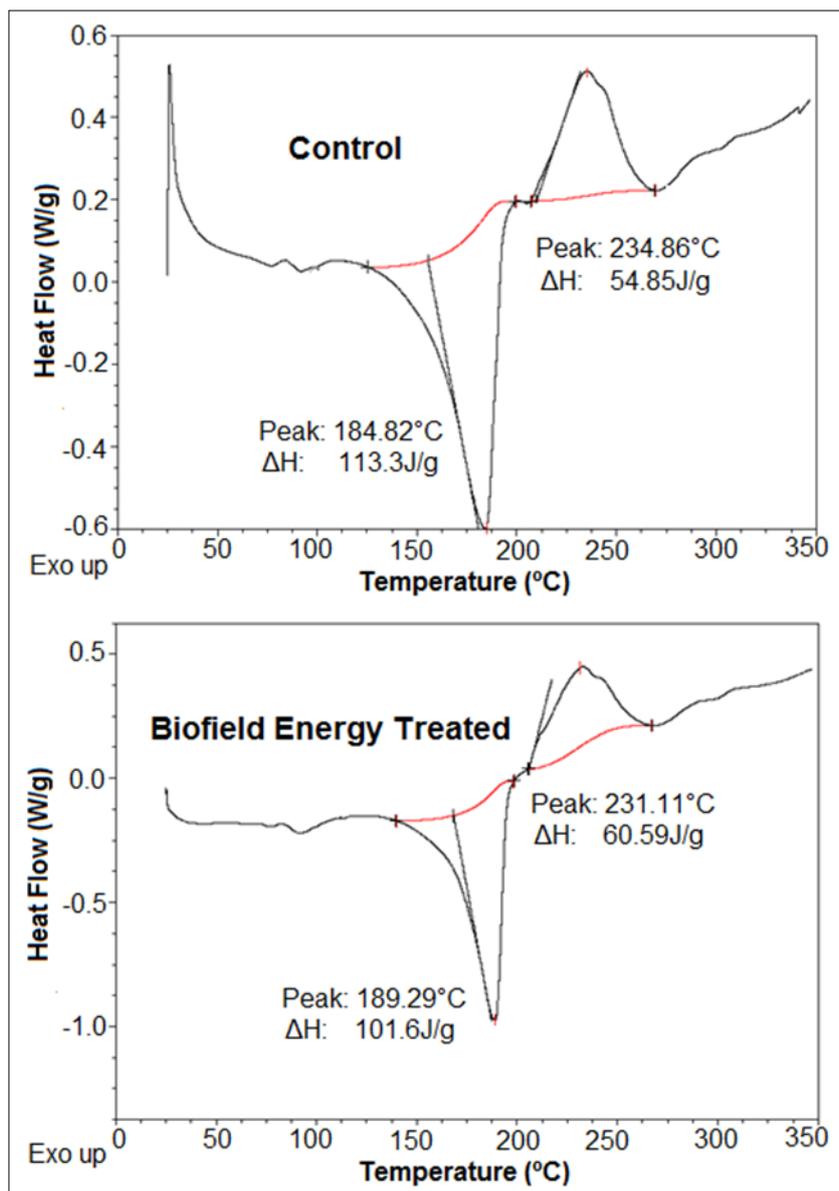


Figure 4. DSC thermograms of the control and the Biofield Energy Treated folic acid.

Table 4. Comparison of DSC data between the control and the Biofield Energy Treated folic acid.

Peak	Description	Melting Point (°C)	ΔH (J/g)
Peak 1	Control sample	184.82	113.30
	Biofield Treated sample	189.29	101.60
	% Change*	2.42	-10.33
Peak 2	Control sample	234.86	54.85
	Biofield Treated sample	231.11	60.59
	% Change*	-1.60	10.46

ΔH: Latent heat of fusion/decomposition; \*denotes the percentage change of the Biofield Energy Treated sample with respect to the control sample.

Trivedi Global, Inc., Trivedi Testimonials, and Trivedi Master Wellness for their assistance and support during this work.

### Conflict of Interest

Authors declare no conflict of interest.

### References

1. Guiland JC, Aimone-Gastin I (2013) Vitamin B<sub>9</sub>. Rev Prat. 63, 1079, 1081-1084.
2. Carmel R (2005) Folic Acid. In: Modern Nutrition in Health and Disease. Shils M, Shike M, Ross A, Caballero B, Cousins R (Ed.) Lippincott Williams & Wilkins, Baltimore, MD.
3. Pobocik RS, Richer JJ (2002) Estimated intake and food sources of vitamin A, folate, vitamin C, vitamin E, calcium, iron, and zinc for Guamanian children aged 9 to 12. Pac Health Dialog. 9, 193-202.
4. Whittaker P, Tufaro PR, Rader JI (2001). Iron and folate in fortified cereals. J Am Coll Nutr. 20, 247-254.
5. Kelly GS (1998) Foliates: Supplemental forms and therapeutic applications. Altern Med Rev. 3, 208-220.
6. Fenech M (2012) Folate (vitamin B<sub>9</sub>) and vitamin B<sub>12</sub> and their function in the maintenance of nuclear and mitochondrial genome integrity. Mutat Res. 733, 21-33.
7. Greenberg JA, Bell SJ, Guan Y, Yu Y (2011) Folic Acid supplementation and pregnancy: More than just neural tube defect prevention. Rev Obstet Gynecol. 4, 52-59.
8. Allen LH (2008) Causes of vitamin B<sub>12</sub> and folate deficiency. Food Nutr Bull. 29, S20-34.
9. Scholl TO, Johnson WG (2000) Folic acid: influence on the outcome of pregnancy. Am J Clin Nutr. 71, 1295S-1303S.
10. Harten P (2005) Reducing toxicity of methotrexate with folic acid. Z Rheumatol. 64, 353-358.
11. Khadka P, Ro J, Kim H, Kim I, Kim JT, et al. (2014) Pharmaceutical particle technologies: An approach to improve drug solubility, dissolution and bioavailability. Asian J Pharm. 9, 304-316.
12. Trivedi MK, Branton A, Trivedi D, Shettigar H, Bairwa K, et al. (2015) Fourier transform infrared and ultraviolet-visible spectroscopic characterization of biofield treated salicylic acid and sparfloxacin. Nat Prod Chem Res. 3, 186.
13. Trivedi MK, Tallapragada RM, Branton A, Trivedi D, Nayak G, et al. (2015) The potential impact of biofield energy treatment on the atomic and physical properties of antimony tin oxide nanopowder. American Journal of Optics and Photonics. 3, 123-128.
14. Warber SL, Cornelio D, Straughn, J, Kile G (2004) Biofield energy healing from the inside. J Altern Complement Med. 10, 1107-1113.
15. Hammerschlag R, Levin M, McCraty R, Bat N, Ives JA, et al. (2015) Biofield Physiology: A Framework for an Emerging Discipline. Glob Adv Health Med. 4, 35-41.
16. Koithan M (2009) Introducing complementary and alternative therapies. J Nurse Pract. 5, 18-20.
17. Trivedi MK, Tallapragada RM, Branton A, Trivedi D, Nayak G, et al. (2015) Spectral and thermal properties of biofield energy treated cotton. American Journal of Energy Engineering. 3, 86-92.
18. Trivedi MK, Patil S, Shettigar H, Bairwa K, Jana S (2015) Effect of biofield treatment on spectral properties of paracetamol and piroxicam. Chem Sci J. 6, 98.
19. Trivedi MK, Branton A, Trivedi D, Nayak G, Mondal SC, et al. (2015) Morphological characterization, quality, yield and DNA fingerprinting of biofield energy treated alphonso mango (*Mangifera indica* L.). Journal of Food and Nutrition Sciences. 3, 245-250.
20. Trivedi MK, Branton A, Trivedi D, Nayak G, Mondal SC, et al. (2015) Evaluation of biochemical marker – Glutathione and DNA fingerprinting of biofield energy treated *Oryza sativa*. American Journal of BioScience. 3, 243-248.
21. Trivedi MK, Branton A, Trivedi D, Nayak G, Charan S, et al. (2015) Phenotyping and 16S rDNA analysis after biofield treatment on *Citrobacter braakii*: A urinary pathogen. J Clin Med Genom. 3, 129.
22. Trivedi MK, Patil S, Shettigar H, Mondal SC, Jana S (2015) Evaluation of biofield modality on viral load

- of Hepatitis B and C viruses. *J AntivirAntiretrovir.* 7, 083-088.
23. Trivedi MK, Patil S, Shettigar H, Mondal SC, Jana S (2015) An impact of biofield treatment: Antimycobacterial susceptibility potential using BACTEC 460/MGIT-TB System. *Mycobact Dis.* 5, 189.
  24. Trivedi MK, Patil S, Shettigar H, Bairwa K, Jana S (2015) Phenotypic and biotypic characterization of *Klebsiella oxytoca*: An impact of biofield treatment. *J MicrobBiochemTechnol.* 7, 203-206.
  25. Nayak G, Altekar N (2015) Effect of biofield treatment on plant growth and adaptation. *J Environ Health Sci.* 1, 1-9.
  26. Trivedi MK, Tallapragada RM (2008) A transcendental to changing metal powder characteristics. *Met Powder Rep.* 63, 22-28, 31.
  27. Trivedi MK, Nayak G, Patil S, Tallapragada RM, Latiyal O (2015) Studies of the atomic and crystalline characteristics of ceramic oxide nano powders after bio field treatment. *IndEng Manage.* 4, 161.
  28. Trivedi MK, Nayak G, Patil S, Tallapragada RM, Latiyal O, et al. (2015) Effect of biofield energy treatment on physical and structural properties of calcium carbide and praseodymium oxide. *International Journal of Materials Science and Applications.* 4, 390-395.
  29. Trivedi MK, Branton A, Trivedi D, Nayak G, Singh R, et al. (2015) Characterization of Physical, Spectral and Thermal Properties of Biofield treated Resorcinol. *Organic Chem Curr Res.* 4,146.
  30. Trivedi MK, Branton A, Trivedi D, Nayak G, Plikerd WD, et al. (2017) A Systematic study of the biofield energy healing treatment on physicochemical, thermal, structural, and behavioral properties of magnesium gluconate. *International Journal of Bioorganic Chemistry.* 2, 135-145.
  31. Trivedi MK, Branton A, Trivedi D, Nayak G, Plikerd WD, et al. (2017) Chromatographic and spectroscopic characterization of the consciousness energy healing treated *Withania Somnifera* (ashwagandha) root extract. *European Journal of Biophysics.* 5, 38-47.
  32. Kinney JP, Trivedi MK, Branton A, Trivedi D, Nayak G, et al. (2017) Overall skin health potential of the biofield energy healing based herbomineral formulation using various skin parameters. *American Journal of Life Sciences.* 5, 65-74.
  33. Branton A, Jana S (2017) The influence of energy of consciousness healing treatment on low bioavailable resveratrol in male *Sprague Dawley* rats. *International Journal of Clinical and Developmental Anatomy.* 3, 9-15.
  34. Branton A, Jana S (2017) The use of novel and unique biofield energy healing treatment for the improvement of poorly bioavailable compound, berberine in male *Sprague Dawley* rats. *American Journal of Clinical and Experimental Medicine.* 5, 138-144.
  35. Branton A, Jana S (2017) Effect of The biofield energy healing treatment on the pharmacokinetics of 25-hydroxyvitamin D<sub>3</sub> [25(OH)D<sub>3</sub>] in rats after a single oral dose of vitamin D<sub>3</sub>. *American Journal of Pharmacology and Phytotherapy.* 2, 11-18.
  36. Koster DA, Trivedi MK, Branton A, Trivedi D, Nayak G, et al. (2018) Evaluation of biofield energy treated vitamin D<sub>3</sub> on bone health parameters in human bone osteosarcoma cells (MG-63). *Biochemistry and Molecular Biology.* 3, 6-14.
  37. Trivedi MK, Patil S, Shettigar H, Gangwar M, Jana S (2015) *In vitro* evaluation of biofield treatment on cancer biomarkers involved in endometrial and prostate cancer cell lines. *J Cancer SciTher.* 7, 253-257.
  38. Trivedi MK, Sethi KK, Panda P, Jana S (2017) Physicochemical, thermal and spectroscopic characterization of sodium selenate using XRD, PSD, DSC, TGA/DTG, UV-vis, and FT-IR. *Marmara Pharmaceutical Journal.* 21/2, 311-318.
  39. Trivedi MK, Sethi KK, Panda P, Jana S (2017) A comprehensive physicochemical, thermal, and spectroscopic characterization of zinc (II) chloride using X-ray diffraction, particle size distribution, differential scanning calorimetry, thermogravimetric analysis/differential thermogravimetric analysis, ultraviolet-visible, and Fourier transform-infrared

- spectroscopy. International Journal of Pharmaceutical Investigation. 7, 33-40.
40. Zhang T, Paluch K, Scalabrino G, Frankish N, Healy AM, et al. (2015) Molecular structure studies of (1S,2S)-2-benzyl-2,3-dihydro-2-(1H-inden-2-yl)-1H-inden-1-ol. J Mol Struct. 1083, 286-299.
41. Desktop X-ray Diffractometer "MiniFlex+". The Rigaku Journal. 14, 29-36, 1997.
42. Langford JI, Wilson AJC (1978) Scherrer after sixty years: A survey and some new results in the determination of crystallite size. J Appl Cryst. 11, 102-113.
43. Trivedi MK, Branton A, Trivedi D, Nayak G, Plikerd WD, et al. (2017) A systematic study of the biofield energy healing treatment on physicochemical, thermal, structural, and behavioral properties of iron sulphate. International Journal of Bioorganic Chemistry. 2, 135-145.
44. Loh ZH, Samanta AK, Heng PWS (2015) Overview of milling techniques for improving the solubility of poorly water-soluble drugs. Asian J Pharm. 10, 255-274.
45. Hu J, Johnston KP, Williams RO (2004) Nanoparticle engineering processes for enhancing the dissolution rates of poorly water soluble drugs. Drug Dev Ind Pharm. 30, 233-245.
46. Trivedi MK, Branton A, Trivedi D, Nayak G, Plikerd WD, et al. (2017) Evaluation of the physicochemical, spectral, thermal and behavioral properties of sodium selenate: influence of the energy of consciousness healing treatment. American Journal of Quantum Chemistry and Molecular Spectroscopy. 2, 18-27.
47. Trivedi MK, Branton A, Trivedi D, Nayak G, Lee AC, et al. (2017) Evaluation of the impact of biofield energy healing treatment (the Trivedi Effect<sup>®</sup>) on the physicochemical, thermal, structural, and behavioural properties of magnesium gluconate. International Journal of Nutrition and Food Sciences. 6, 71-82.
48. Gill P, Moghadam TT, Ranjbar B (2010) Differential Scanning Calorimetry Techniques: Applications in Biology and Nanoscience. J Biomol Tech. 21, 167-193.
49. Gazzali AM, Lobry M, Colombeu L, Acherar S, Azais H, et al. (2016) Stability of folic acid under several parameters. Eur J Pharm Sci. 93, 419-430.
50. Zhao Z, Xie M, Li Y, Chen A, Li G, et al. (2015) Formation of curcumin nanoparticles *via* solution enhanced dispersion by supercritical CO<sub>2</sub>. Int J Nanomedicine. 10, 3171-3181.